Spatial dynamics of solitonlike channels near interfaces between optically linear and nonlinear media

Yu. M. Aliev,[1] A. D. Boardman,[2] A. I. Smirnov,[3] K. Xie,[2] and A. A. Zharov[3]
[1]*P. N. Lebedev Physical Institute, Russian Academy of Sciences, 53 Leninsky Prospect, 117924, Moscow, Russia*
[2]*Joule Laboratory, Department of Physics, University of Salford, Salford M5 4WT, United Kingdom*
[3]*Institute of Applied Physics, Russian Academy of Sciences, 46 Uljanov Street, 603600, Nizhny Novgorod, Russia*
(Received 17 July 1995; revised manuscript received 10 January 1996)

The present paper is devoted to an investigation of the influence of *radiative losses* upon the spatial dynamics of *self-consistent* waveguide channels that are localized near interfaces between linear and Kerr-type nonlinear dielectric media. It is shown that the radiative effects, through their dependence on the intensity of the electromagnetic fields, the initial channel position, and its angle of inclination to an interface, can lead either to the total disappearance of a nonlinear channel formation, or to its displacement, deep into the nonlinear medium, as a consequence of the loss of some part of the initial energy. The nonlinear interaction of self-consistent channels with externally incident, stimulating, beams is studied, and stability of the resulting steady states is determined. In order to carry out these investigations, an original approach is used that is based on the assumption of a small overlap between externally incident waves and the internal, nonlinear, quasilocalized eigenmode. It is shown that this method permits equations to be obtained that determine the spatial dynamics of channel energy, and position, together with the structure of the scattered field. [S1063-651X(96)09305-1]

PACS number(s): 42.25.Gy

I. INTRODUCTION

The interaction of strong electromagnetic fields with nonlinear/nonlinear or linear/nonlinear interfaces, generated with dielectric media, is an important area of modern optics. One of the most interesting aspects of such problems is the penetration of radiation into a nonlinear medium with subsequent self-focusing properties, when wave packets are incident upon a linear/nonlinear interface, at an angle greater than is necessary for total internal reflection. Within the framework of an elegant stationary state theory, using plane waves, Kaplan [1–6] predicted the appearance of optical bistability in the reflectivity, and stimulated transparency. These papers led to activity which is still vigorous today. Bistable effects were soon observed [7], and the transparency threshold of a nonlinear medium was measured. Indeed, an even earlier prediction [8] that the stationary, spatially homogeneous, transparency regime of a self-focusing medium is unstable is now accepted as well known. It follows from this property that, when certain power thresholds are exceeded, by increasing the amplitude of a wave incident upon an interface between linear and nonlinear media, a dynamic, or inhomogeneous, superthreshold regime will occur. In fact, the first two-dimensional numerical calculations of the reflection of a plane wave in this superthreshold regime [9] showed that an electromagnetic field penetrates into the nonlinear medium in the form of self-sustaining channels (filaments). These channels form a periodic grating, whose period depends upon how much the incident wave amplitude exceeds the threshold value. The reflected field, on the other hand, assumes the form of *electromagnetic jets*. Very recent theoretical investigations show [10] that transparency can also occur together with the periodic generation of solitons, which run deep into the nonlinear medium, or are accompanied by a more complicated, spatially inhomogeneous, dynamic regime. In this context, it is interesting that numerical calculations of stationary scattering of wave beams by nonlinear interfaces [9–14] reveal the presence of filamentation of transmitted radiation that look rather like the plane wave case, at higher thresholds. For this case, the number of filaments depends upon the superthreshold value of the incident radiation. The possibility of a giant, nonlinear, shift of the center of gravity of the reflected beam can also be demonstrated [9–14]. This giant shift, in contrast to the well-known linear Goos-Hänchen effect [15,16], can be much greater than the incident beam width. In some papers [14,17], such a giant nonlinear Goos-Hänchen effect is associated with the excitation of the unstable branch of a nonlinear surface wave [18–22], but, in the paper by Aliev *et al.* [10], the giant Goos-Hänchen effect is explained in terms of the excitation of a near-surface, nonlinear, weakly radiative, self-consistent channel (nonlinear quasilocalized mode) that provides an electromagnetic energy transfer along the interface. Also, the trajectories of the excited self-consistent channels are very sensitive [10] to any changes in the parameters of the incident radiation, such as amplitude, angle of incidence and beam width variation.

It is clear, then, that the scattering of wave beams, which are incident upon the interface between a linear and a nonlinear medium, at angles of incidence greater than the critical one for total internal reflection, is determined by the nature of the interaction between self-consistent waveguides excited into nonlinear medium and any pump wave. The scattering is also determined by energy emission from them, through the interface. It is important to note, however, that self-consistent channels have a width that is of the order of the dimension of the skin layer, and that it is weakly coupled to the pump wave. It is necessary, therefore, to investigate the spatial dynamics of nonlinear self-focused waveguides that

have small radiation losses in the presence of a pump wave, as well as in the free-emission regime. In this connection, as far as analytical results currently available in the literature [23,25] are concerned, it appears that they deal with the solution of very specific problems. In particular, they involve the interaction (reflection and transmission) of self-consistent channels with the interface between two nonlinear Kerr-like media which have very similar physical properties, and are close enough to each other for an equivalent particle method to be used. The interface in such theories [23–26] is considered to be a small perturbation to the nonlinear Schrödinger equation, and the transverse structure of the channels is assumed to be invariant. In spite of the fact that this interesting theoretical approach [23–26] does predict a number of important effects, it has to be admitted that it cannot be applied to problems involving wide wave packet scattering by nonlinear interfaces, because of the nonradiative character of the channel, or to an interface between media with widely differing nonlinear properties. Recent theory, based upon an energy transfer equation [10], does account for such strongly differing properties, by dealing with a linear/nonlinear interface, and the generation of filaments and soliton formation in the vicinity of the skin layer. However, it does not include any interaction of the channels with the pump wave, after the channels are created.

The purpose of this paper, therefore, is to study the dynamics of such radiatively damped self-consistent waveguide channels, in the field of incident wave beams that could be quite wide. The theory will embrace cases which involve interfaces between media with widely differing properties, and include an analysis of the stability of the steady states. The existence of small overlap parameters conveniently presents the possibility of using another kind of perturbation theory, as suggested in an earlier paper [27]. Here the theory deals with phase-matched interaction between the radiation fields, and quasilocalized nonlinear modes. Although this approach may look somewhat like the perturbation theory developed for certain soliton dynamics problems (see, for example, [28–30]), it differs from it, in an essential way, by taking into account radiation effects, analyzed within the framework of the theory suggested earlier in this introduction. It permits, in practice, the calculation of the trajectories of the waveguide channels, the change in the energy flow in them due to emission and pumping, and the determination of the structure of the radiated fields. The results obtained enable an interpretation of some effects that, up to now, are only capable of demonstration by extensive two-dimensional (2D) numerical calculations.

II. BASIC EQUATIONS AND PERTURBATION THEORY

A planar interface between a linear and a nonlinear medium is shown in Fig. 1. The nonlinear medium that occupies the $z>0$ half-space is Kerr-like, with a dielectric permittivity that depends upon the intensity of the electromagnetic wave field $\mathscr{E}$. The dielectric functions are ε_1=cons (linear medium) $\varepsilon(|\mathbf{E}(\omega)|^2)$ (nonlinear medium), and the electric field $\mathscr{E}$ is

$$\mathscr{E}=\tfrac{1}{2}[\mathbf{E}(\omega)e^{-i\omega t}+\text{c.c.}],$$

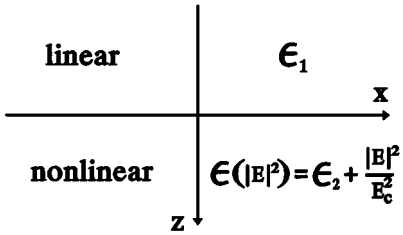

FIG. 1. The linear/nonlinear interface.

where ω is the angular frequency, $\mathbf{E}(\omega)\equiv\mathbf{E}$ is the Fourier amplitude of the electric field, and c.c. denotes the complex conjugate. Only a nonlinear medium with self-focusing properties is going to be considered here, so that

$$\frac{\partial\varepsilon}{\partial|E|^2}>0,$$

In order to be specific, it is assumed that $\varepsilon_1>\varepsilon_2=\varepsilon(|\mathbf{E}|^2=0)$, and that the wave fields are *s* polarized, i.e., $\mathbf{E}=E\hat{\mathbf{y}}$, where $\hat{\mathbf{y}}$ is a unit vector along the *y* direction. The basic wave equation is now

$$\nabla^2E+k_0^2\varepsilon_T(z,|E|^2)E=0, \tag{1}$$

where $\nabla^2=(\partial^2/\partial x^2)+(\partial^2/\partial z^2)$, $k_0=\omega/c$ is the free-space wave number, $\partial/\partial y=0$, c is the speed of light in a vacuum, and the dielectric function of the whole interface structure is

$$\varepsilon_T(z,|E|^2)=\begin{cases}\varepsilon_1, & z<0\\ \varepsilon(|E|^2)=\varepsilon_2+\dfrac{|E|^2}{E_c^2}, & z>0,\end{cases} \tag{2}$$

where $1/E_c^2$ is the coefficient of nonlinearity and ε_2 is the linear part of $\varepsilon(|\mathbf{E}|^2)$.

The field E can be split, formally, into two parts E_1 and E_2, i.e., $E=E_1+E_2$, where the separate parts satisfy the equations

$$\nabla^2E_1+\varepsilon^LE_1=-[\varepsilon_T-\varepsilon(|\mathbf{E}|^2)]E_2\equiv F_1, \tag{3a}$$

$$\nabla^2E_2+\varepsilon(|\mathbf{E}|^2)E_2=-[\varepsilon_T-\varepsilon^L]E_1\equiv F_2, \tag{3b}$$

in which the transformations $x\to k_0x, z\to k_0z$ have been made, and the linear part of ε_T is $\varepsilon^L=\varepsilon_1$, if $z<0$, and $\varepsilon^L=\varepsilon_2$, if $z>0$. Each part of E is *driven* by the terms F_1 and F_2, which are defined as

$$F_1=0,\quad F_2=-\frac{|E|^2}{E_c^2}E_1,\quad z>0, \tag{4a}$$

$$F_2=0,\quad F_1=-(\varepsilon_1-\varepsilon_2)E_2,\quad z<0. \tag{4b}$$

The interpretation of Eqs. (3) is as follows. The solutions of the homogeneous equations ($F_1=0$, $F_2=0$) are $E_1^{(0)}$ and $E_2^{(0)}$, respectively. The $E_1^{(0)}$ field *alone* is a plane wave traveling in an entirely linear medium. It travels toward the interface in the region $z<0$ and totally internally reflects at the $z=0$ interface between this region and a $z>0$, *nonlinear* semi-infinite, half-space. $E_1^{(0)}$ has, therefore, only a small exponential tail reaching into this $z>0$ half-space. The $E_2^{(0)}$ field *alone* arises from a self-focused beam traveling in a nonlinear medium, parallel to the interface, and it, too, has only a

weak exponential tail but, this time, stretching into the linear $z<0$ lower half-space. From this information it can be appreciated that F_2 and F_1 can be treated as perturbations; i.e., in the actual system, the *tail* of the self-focused wave, in $z<0$, *perturbs* $E_1^{(0)}$ to E_1, and the *tail* of the incoming wave, reflected at $z=0$, *perturbs* $E_2^{(0)}$ to E_2. Note that it is not necessary to require both half-spaces to be nonlinear in order to apply this perturbative method.

The first task is to determine the homogeneous solutions $E_1^{(0)}$ and $E_2^{(0)}$. For this model, $E_1^{(0)}$ is a plane wave incident upon the $z=0$ interface, at an angle greater than the critical angle. For $F_1=0$, the $E_1^{(0)}$ wave propagating toward the interface has a wave vector $\mathbf{k}=(k_x,k_z)$, where $k_x=\gamma$ and $k_z=\kappa_1$ (scaled with k_0). In the $z>0$ half space there is exponential decay, and $k_x=\gamma$, and $k_z=i\kappa_2$. Hence $\kappa_1=\sqrt{\varepsilon_1-\gamma^2}$, $\kappa_2=\sqrt{\gamma^2-\varepsilon_2}$, and

$$E_1^{(0)}=\begin{cases} C\ \exp(-\kappa_2 z-i\gamma x), & z>0 \\ A_0\ \exp(i\phi_0-i\kappa_1 z-i\gamma x), & \\ +B\ \exp(i\kappa_1 z-i\gamma x) & z<0 \end{cases} \quad \text{for } F_1=0, \quad (5)$$

where it is convenient to use a *real* amplitude A_0 for the incident plane wave, together with ϕ_0 (=const) as a phase factor. This representation is convenient for the subsequent analysis of channel dynamics in the nonlinear medium, as will be made clear below. B, the complex amplitude of the reflected wave, is

$$B=\left(\frac{i\kappa_1-\kappa_2}{i\kappa_1+\kappa_2}\right)A_0\exp(i\phi_0), \quad (6)$$

and C, the amplitude of electric field at the interface $z=0$, is

$$C=\frac{2i\kappa_1}{i\kappa_1+\kappa_2}A_0\exp(i\phi_0). \quad (7)$$

A finite beam can be represented as an integral over *all* the plane waves that make up the beam. If such a beam width is large enough to ensure that

$$k_0 a_\perp \gg 1, \quad \theta-\theta_c \gg \delta\theta,$$

where $\delta\theta$ is the angle of incidence spread of the plane-wave bundle making up the beam, $a_\perp$ is the transverse dimension of the beam, θ is the angle of incidence to the normal, and θ_c is the critical angle for total internal reflection, ($\theta_c=\sin^{-1}\sqrt{\varepsilon_2/\varepsilon_1}$). Then A_0 should be replaced by slowly varying functions $A_0(x)$ and $\phi_0(x)$. These are functions that characterize the amplitude distribution and the phase front of the beam at the interface, and will be introduced below.

The solution $E_2^{(0)}$ of the homogeneous part of Eq. (3b) can be easily found by setting $F_2=0$ and decoupling (3b) from (3a) by setting $\varepsilon(|E|^2)=\varepsilon(|E_2|^2)$. After these actions are taken, Eq. (3b) has the standard solution

$$E_2^{(0)}=\psi_0\exp(-i\gamma_s^{(0)}x), \quad \psi_0=\frac{\sqrt{2}\kappa_2^{(s0)}E_c}{\cosh[\kappa_2^{(s0)}(z-z_0)]} \quad \text{for } F_2=0, \quad (8)$$

where $\kappa_2^{(s0)^2}=\gamma_s^{(0)^2}-\varepsilon_2$, and $\gamma_s^{(0)}$ is the component of the wave number along the interface for an *isolated* self-focused beam. The superscript (0) is introduced to label this as a stationary state and s labels the solution as an induced waveguide channel (soliton). Up to now, only the *independent* solutions $E_1^{(0)}$ and $E_2^{(0)}$, shown in Fig. 2 to emphasize their character, have been derived and they are associated, respectively, with x components of the wave vectors equal to γ and $\gamma_s^{(0)}$. The task now is to couple the radiation field and the localized beam. In order to achieve this, it will be assumed that the self-focused channel (quasisurface wave) is localized at a distance z_0 from the interface, where z_0 exceeds the channel width. This means that in the coupled nonstationary regime $|E_2(z=0)|\ll|E_2(z=z_0)|$, and that $\varepsilon(|E(z=0)|^2)\approx\varepsilon_2$. The solutions of Eqs. (3a) and (3b) are $E_1\neq E_1^{(0)}$ and $E_2\neq E_2^{(0)}$ because the *driving terms* F_1 and F_2 are now taken into account. For example, Eq. (3a) is inhomogeneous with a *source term* F_1 localized in the $z<0$ half-space, and the solutions to (3a) and (3b) can be found by exploiting a weak overlap approximation. The incoming radiation field in the linear half-space creates a rapidly decaying field in the nonlinear medium, so F_2 is very small in the region where the soliton channel is heavily localized. Similarly, because the beam is localized in a position at least one beam width away from the surface, the *tail* of its field in the linear half-space is also very weak. Hence it is emphasized, once again, that F_1, the driving term in (3a), is a perturbation term.

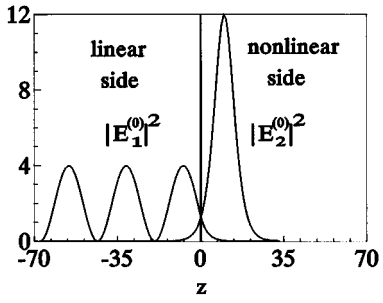

FIG. 2. Unperturbed field amplitude structures $|E_1^{(0)}|^2$ and $|E_2^{(0)}|^2$, in dimensionless units, for a single interface system.

The $E_1^{(0)}$ field is perturbed to E_1, and its structure is as follows. For $z>0$, there will be the contribution given in Eq. (5) plus a perturbation varying as $\exp[-\kappa_2^{(s)}z-i\gamma_s x]$. In the absence of the incoming plane wave field, in the linear half-space, the self-focused beam would have a wave number $\gamma_s^{(0)}$, but in the presence of this pump field it has a different wavenumber γ_s. For $z<0$, E_1 has parts given by Eq. (5) plus a *radiation term* $\exp[i\kappa_1^{(s)}z-i\gamma_s x]$, caused by the beam and a *beam tail* term $\exp[\kappa_2^{(s)}(z-z_0)-i\gamma_s x]$. Note that $F_1=0$, for $z>0$, and $E_2^{(0)}\approx 2\sqrt{2}\kappa_2^{(s)}e^{\kappa_2^{(s)}(z-z_0)-i\gamma_s x}E_c$ in the $z<0$ region, so taking all the above points into account shows that the field E_1 is

$$E_1=\begin{cases} Ce^{-\kappa_2 z-i\gamma x}+Qe^{-\kappa_2^{(s)}z-i\gamma_s x}, & z>0 \\ A_0e^{i\phi_0-i\kappa_1 z-i\gamma x}+Be^{i\kappa_1 z-i\gamma x}+Ge^{i\kappa_1^{(s)}z-i\gamma_s x} & \\ \quad +De^{\kappa_2^{(s)}(z-z_0)-i\gamma_s x}, & z<0, \end{cases} \quad (9)$$

where, at this stage, γ and γ_s are not functions of the propagation distance x. The substitution of solutions (9) into Eq. (3a) yields the following relationships:

$$D=-2\sqrt{2}\kappa_2^{(s)}E_c,$$

$$Q=2\sqrt{2}\kappa_2^{(s)}\,\frac{\kappa_2^{(s)}-i\kappa_1^{(s)}}{\kappa_2^{(s)}+i\kappa_1^{(s)}}\,e^{-\kappa_2^{(s)}z_0}E_c, \tag{10}$$

$$G=4\sqrt{2}\,\frac{{\kappa_2^{(s)}}^2}{\kappa_2^{(s)}+i\kappa_1^{(s)}}\,e^{-\kappa_2^{(s)}z_0}E_c.$$

Also,

$${\kappa_2^{(s)}}^2-\gamma_s^2+\varepsilon_2=0,\quad {\kappa_1^{(s)}}^2+\gamma_s^2-\varepsilon_1=0.$$

The stationary state $E_2=E_2^{(0)}$ is given by Eq. (8) but, when $F_2\neq 0$, the following nonstationary state $E_2=\psi e^{-i\gamma_s^{(0)}x}$ can be used, where

$$\psi=\frac{\sqrt{2}\kappa_2^{(s)}E_c}{\cosh[\kappa_2^{(s)}(z-z_0)]}\times\exp\left\{-i\int[\gamma_s-\gamma_s^{(0)}]dx-ia(z-z_0)\right\}, \tag{11}$$

in which a, z_0, $\kappa_2^{(s)}$, and γ_s are to be determined. a is a phase change producing a *small* noncollinearity of the channel axis and the interface direction, and $\kappa_2^{(s)}$ is different from $\kappa_2^{(s0)}$ because it is the *nonstationary* value. Equation (11) immediately yields

$$\int|\psi|^2dz=4E_c^2\kappa_2^{(s)}, \tag{12a}$$

$$\int\psi z\psi^*dz=4E_c^2\kappa_2^{(s)}z_0, \tag{12b}$$

$$i\int\left[\psi^*\frac{\partial\psi}{\partial z}-\frac{\partial\psi^*}{\partial z}\psi\right]dz=8a\kappa_2^{(s)}E_c^2, \tag{12c}$$

and Eq. (3b) becomes

$$-2i\gamma_s^{(0)}\frac{\partial\psi}{\partial x}+\frac{\partial^2\psi}{\partial z^2}+\left[\frac{|\psi|^2}{E_c^2}-{\kappa_2^{(s0)}}^2\right]\psi=F_2e^{i\gamma_s^{(0)}x}. \tag{13}$$

The differential of Eq. (12a), with respect to x, is

$$\frac{d\kappa_2^{(s)}}{dx}=\frac{1}{4E_c^2}\int\left[\frac{d\psi}{dx}\psi^*+\psi\frac{d\psi^*}{dx}\right]dz, \tag{14}$$

so the substitution of $d\psi/dx$ and $d\psi^*/dx$, from Eq. (13), gives

$$\frac{d\kappa_2^{(s)}}{dx}=\frac{i}{8E_c^2\gamma_s^{(0)}}\int[F_2\exp(i\gamma_s^{(0)}x)\psi^*-F_2^*\exp(-i\gamma_s^{(0)}x)\psi]dz. \tag{15}$$

From Eqs. (2), (4a), (9), and (11), for the region $z>0$,

$$F_2e^{i\gamma_s^{(0)}x}\psi^*=-\frac{|\psi|^3}{E_c^2}e^{-\kappa_2^{(s)}z}[Ce^{-i\int\gamma dx}+Qe^{-i\int\gamma_s dx}]\times e^{i\int\gamma_s dx+ia(z-z_0)}=-\frac{1}{E_c^2}[Ce^{i\phi}+Q]|\psi|^3e^{-\kappa_2^{(s)}z+ia(z-z_0)}, \tag{16}$$

where $\phi=\int(\gamma_s-\gamma)dx$. Hence, since a is small, Eq. (15) can be written as

$$\frac{\gamma_s}{\kappa_2^{(s)}}\frac{d\gamma_s}{dx}=\frac{q_2}{4E_c^4\gamma_s^{(0)}}\,\mathrm{Im}[Ce^{i\phi}+Q], \tag{17}$$

where $\kappa_2^{(s)}d\kappa_2^{(s)}=\gamma_s d\gamma_s$, Im means take the imaginary part, and

$$q_2\approx\int_0^\infty|\psi|^3\exp(-\kappa_2^{(s)}z)dz\approx 4\sqrt{2}{\kappa_2^{(s)}}^2\exp(-\kappa_2^{(s)}z_0)E_c^3, \tag{18}$$

The differential of Eq. (12b), with respect to x, is

$$\frac{d}{dx}(\kappa_2^{(s)}z_0)=\frac{1}{4E_c^2}\int\left[\frac{d\psi}{dx}z\psi^*+\psi z\frac{d\psi^*}{dx}\right]dz. \tag{19}$$

This, through the use of Eq. (13), becomes

$$\frac{d}{dx}(\kappa_2^{(s)}z_0)=\frac{i}{8E_c^2\gamma_s^{(0)}}\int[F_2\exp(i\gamma_s^{(0)}x)\psi^*-F_2^*\exp(-i\gamma_s^{(0)}x)\psi]z\,dz+\frac{i}{8E_c^2\gamma_s^{(0)}}\int\left\{\frac{\partial}{\partial z}\left[\left(\frac{\partial\psi^*}{\partial z}\psi-\frac{\partial\psi}{\partial z}\psi^*\right)z\right]-\left(\frac{\partial\psi^*}{\partial z}\psi-\frac{\partial\psi}{\partial z}\psi^*\right)\right\}dz. \tag{20}$$

The integrations

$$\int[F_2\exp(i\gamma_s^{(0)}x)\psi^*-F_2^*\exp(-i\gamma_s^{(0)}x)\psi](z-z_0)dz\cong 0,$$

$$\int\frac{\partial}{\partial z}\left[\left(\frac{\partial\psi^*}{\partial z}\psi-\frac{\partial\psi}{\partial z}\psi^*z\right)\right]dz=0,$$

together with Eq. (12c), reduce Eq. (20) to

$$\kappa_2^{(s)}\frac{dz_0}{dx}+z_0\frac{d\kappa_2^{(s)}}{dx}=z_0\frac{d\kappa_2^{(s)}}{dx}+a\frac{\kappa_2^{(s)}}{\gamma_s^{(0)}},$$

so that

$$\frac{dz_0}{dx}=\frac{a}{\gamma_s^{(0)}}, \tag{21}$$

Equation (12c) gives

$$\frac{d}{dx}(a\kappa_2^{(s)}) = \frac{i}{8E_c^2}\int\left[\frac{\partial\psi}{\partial z}\frac{\partial\psi^*}{\partial x}+\psi^*\frac{\partial^2\psi}{\partial x\partial z}-\psi\frac{\partial^2\psi^*}{\partial x\partial z} - \frac{\partial\psi^*}{\partial z}\frac{\partial\psi}{\partial x}\right]dx. \tag{22}$$

The use of Eq. (13), in Eq. (22) gives

$$\frac{d}{dx}(a\kappa_2^{(s)}) = \frac{1}{8E_c^2\gamma_s^{(0)}}\int F_2\frac{d|\psi|}{dz}\exp(i\gamma_s^{(0)}x) \times\exp\left[i\int(\gamma_s-\gamma_s^{(0)})dx+ia(z-z_0)\right]dz + \frac{ia}{8E_c^2\gamma_s^{(0)}}\int F_2\exp(i\gamma_s^{(0)}x)\psi^*dz+\text{c.c.}, \tag{23}$$

where c.c. denotes the complex conjugate.

The first term in Eq. (23) is

$$\int F_2\frac{d|\psi|}{dz}\exp(i\gamma_s^{(0)}x)\exp\left[i\int(\gamma_s-\gamma_s^{(0)})dx+ia(z-z_0)\right] = -\frac{q_1}{E_c^2}[Ce^{i\phi}+Q], \tag{24}$$

and the second term, plus its complex conjugate, is simply $a(d\kappa_2^{(s)}/dx)$. Equation (23), after using Eq. (21), therefore reduces to

$$\gamma_s^{(0)^2}\frac{d^2z_0}{dx^2} = \frac{-q_1}{4E_c^4\kappa_2^{(s)}}\text{Re}[Ce^{i\phi}+Q], \tag{25}$$

where

$$q_1 \approx \int_0^\infty|\psi|^2\frac{d|\psi|}{dz}\exp(-\kappa_2^{(s)}z)dz \approx \tfrac{4}{3}\sqrt{2}\kappa_2^{(s)^3}\exp(-\kappa_2^{(s)}z_0)E_c^3. \tag{26}$$

In summary, this section contains equations that govern the dynamics of a self-consistent waveguide near an interface. The analysis permits the determination of channel trajectories and takes into account the changes of the energy flow in them, resulting from radiative losses and pumping. The structure of the output field is given by Eq. (9).

The rate of change of the energy flow P_s in a self-focused channel with propagation distance x is equal to the outflow of energy radiated into the linear half-space. The energy flow in a channel is

$$P_s = \gamma_s\int_{-\infty}^{\infty}|\psi|^2dz = 4\gamma_s(\gamma_s^2-\varepsilon_2)^{1/2}E_c^2, \tag{27}$$

and

$$\frac{dP_s}{dx} = \frac{4E_c^2}{\gamma_s^{(0)}\sqrt{\gamma_s^2-\varepsilon_2}}\frac{d\gamma_s}{d\eta}\{2\gamma_s^2-\varepsilon_2\}, \tag{28}$$

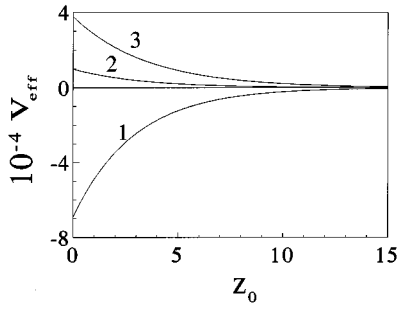

FIG. 3. The effective potential V_{eff} as a function of beam position z_0, for different values of γ_s. (1) $\gamma_s>\gamma_s^*$: attractive potential. (2) and (3) $\gamma_s<\gamma_s^*$: repulsive potentials, where γ_s for (2) is larger than for (3).

III. DYNAMICS OF SELF-CONSISTENT WAVEGUIDE CHANNELS: ZERO PUMP WAVE

In this section, the free motion of self-consistent (self-focused) waveguide channels is investigated. The free motion occurs when the pump field is absent i.e., $A_0=0$. This means that $B=C=0$, and Eqs. (17) and (25) simply become

$$\gamma_s^{(0)^2}\frac{d^2z_0}{dx^2} = -\frac{4}{3}\frac{\kappa_2^{(s)^3}(\kappa_2^{(s)^3}-\kappa_1^{(s)^3})}{(\varepsilon_1-\varepsilon_2)}\exp\{-2\kappa_2^{(s)}z_0\} = -\frac{\partial V_{\text{eff}}}{\partial z_0}, \tag{29a}$$

where V_{eff} is an effective potential, and

$$\gamma_s^{(0)}\gamma_s\frac{d\gamma_s}{dx} = -8\frac{\kappa_1^{(s)}\kappa_2^{(s)^5}}{\varepsilon_1-\varepsilon_2}\exp\{-2\kappa_2^{(s)}z_0\}. \tag{29b}$$

It is interesting that at $\kappa_2^{(s)}=\kappa_1^{(s)}$ there is a change from attraction to repulsion between the beam and the interface. The right-hand part of Eq. (29b) is always negative, and this corresponds to the fact that γ_s is decreasing, which shows that there is a decrease of energy flow in the channel. The only possible physical process that provides such an outflow of energy is *emission* into the linear medium. In fact, Eq. (29a) describes the dynamics of an equivalent quasiparticle, incorporating a radiation reaction, moving in the field of a time-dependent potential (see the right-hand part), which determines the character of the interaction with the interface. Some forms of the effective potential, $V_{\text{eff}}=-\frac{2}{3}(\kappa_2^{(s)^3}[\kappa_2^{(s)^2}-\kappa_1^{(s)^2}])/(\varepsilon_1-\varepsilon_2)\exp[-2\kappa_2^{(s)}z_0]$ for different values of γ_s are shown in Fig. 3. If $\kappa_2^{(s)}>\kappa_1^{(s)}$, or $\gamma_s^2>\frac{1}{2}(\varepsilon_1+\varepsilon_2)=\gamma_s^{*2}$, the interaction of the channel with the interface is attractive (normal refraction). In the opposite case, when $\kappa_2^{(s)}<\kappa_1^{(s)}(\gamma_s^2<\gamma_s^{*2})$, repulsion occurs (anomalous refraction). Hence only channels with large enough energy flow are attracted to the interface. This energy determines the emission angle of the output radiation into the linear medium. In the attractive case, the angle of emission lies in the band,

$$\frac{\pi}{2}>\theta>\theta^*=\sin^{-1}\left\{\left[\frac{1}{2}\left(1+\frac{\varepsilon_2}{\varepsilon_1}\right)\right]^{1/2}\right\},$$

In the repulsive regime, the angle of emission is determined by the inequality

$$\theta^* > \theta > \theta_c .$$

Taking into account the fact that the propagation of radiation in the near-surface channel is accompanied by losses, the character of the interaction will change when the energy flow falls below a critical value. The initial conditions (channel position, angle of inclination to the interface, and energy) define the power and value of the emitted energy.

In order to analyze Eqs. (29) more easily, consider the case when the media have linear dielectric permittivities that are quite close to each other, i.e., $\varepsilon_1-\varepsilon_2 \ll \varepsilon_1,\varepsilon_2$. In this regime, strong simplifications become possible. After introducing the variable $\eta = x/\gamma_s^{(0)}$, Eqs. (20) transform to

$$\frac{d^2 z_0}{d\eta^2} = -\frac{4}{3}\frac{\kappa_2^{(s)^3}(\kappa_2^{(s)^2}-\kappa_1^{(s)^2})}{\Delta\varepsilon}\exp\{-2\kappa_2^{(s)} z_0\}, \quad (30a)$$

$$\frac{d\gamma_s}{d\eta} = -\frac{8\kappa_1^{(s)}\kappa_2^{(s)^2}}{\gamma_s}\left(\frac{\kappa_2^{(s)^3}}{\Delta\varepsilon}\right)\exp\{-2\kappa_2^{(s)} z_0\}, \quad (30b)$$

where $\Delta\varepsilon = \varepsilon_1-\varepsilon_2$. It is immediately apparent that Eq. (30a) can be integrated once, and the pair of equations can then be put in the form

$$\frac{dz_0}{d\eta} = -\frac{1}{12}\left[4\sqrt{\varepsilon_1-u} + \sqrt{\Delta\varepsilon}\,\log\frac{2\varepsilon_1-\varepsilon_2-u-2\sqrt{\Delta\varepsilon(\varepsilon_1-u)}}{u-\varepsilon_2}\right] + \text{const},$$

$$\frac{du}{d\eta} = -\frac{16}{\Delta\varepsilon}(u-\varepsilon_2)^{5/2}(\varepsilon_1-u)^{1/2}\exp(-2z_0\sqrt{u-\varepsilon_2}), \quad (31)$$

where $u=\gamma_s^2$. The constant of integration is determined by u_0, the *initial* value of u, and $(dz_0/d\eta)_0$, the *initial* value of the derivative $dz_0/d\eta$. Hence

$$\frac{dz_0}{d\eta} = -\frac{1}{12}\left\{4(\sqrt{\varepsilon_1-u}-\sqrt{\varepsilon_1-u_0}) + \sqrt{\Delta\varepsilon}\,\log\left[\frac{(2\varepsilon_1-\varepsilon_2-u-2\sqrt{\Delta\varepsilon(\varepsilon_1-u)})(u_0-\varepsilon_2)}{(2\varepsilon_1-\varepsilon_2-u_0-2\sqrt{\Delta\varepsilon(\varepsilon_1-u_0)})(u-\varepsilon_2)}\right]\right\} + \left(\frac{dz_0}{d\eta}\right)_0, \quad (32a)$$

$$\frac{du}{d\eta} = -\frac{16}{\Delta\varepsilon}(u-\varepsilon_2)^{5/2}(\varepsilon_1-u)^{1/2}\exp(-2z_0\sqrt{u-\varepsilon_2}), \quad (32b)$$

where u lies in the range $\varepsilon_2 < u < \varepsilon_1$. Equations (32) permit a qualitative investigation, beginning with the observation that Eq. (32b) describes the radiative emission of energy from the channel and is expressed by the monotonic decrease of the parameter u.

Detailed computer investigations have been carried out of (1) the trajectories (z_0,η) of the center of the self-focused channel waveguides, and (2) the changes in the energy, P_s/P_0, as a function of η, along these trajectories. Some specimen results are displayed in Fig. 4 for a single interface involving media in which the critical angle for total internal reflection is $\theta_c \approx 81.85°$. If a soliton channel propagates toward the interface and is eventually pushed out completely into the linear medium, a special treatment is needed. When the channel center is nearer to the interface than the transverse extent of its localized field, the interaction with the interface is not weak, and perturbation theory of this kind cannot be applied. This fact has been taken into account in the calculations reported here, and the typical initial distance of the beam center from the interface has been set equal to, or beyond $1/(2\kappa_2^{(s)})$, i.e., well beyond the skin depth. Figure 4(a) is a plot of the guide center, z_0, starting from $x=0$. For $u_0=2.67$, $u_0^* = \gamma_s^{*2} = 2.6602$, it is the trajectories of channels which are originally located in the nonlinear medium at $z_0=20$ that are shown in Fig. 4(a) for different initial angle values $(dz_0/d\eta)_0$. Trajectories 1 and 2 show that the solitons are attracted to the interface to begin with, but are repulsed at larger values of x after losing a part of their energy. Trajectory 3 takes off immediately into the nonlinear medium. In the latter case, the energy losses are small, so any attraction does not change the sign of the effective potential. The parts of the trajectories far from the interface suffer very little radiative loss and, therefore, experience almost no interaction with the interface. In more detail, for trajectories 1 and 2 there is an initial fall in P_s followed by a penetration of the channel into the nonlinear medium. When this happens P_s eventually settles down to a constant value. Channel 3 takes off into the nonlinear medium, emitting very little radiation, and, for this case, P_s remains almost constant. Figure 5 shows a beam propagation simulation corresponding to curves 1 of Fig. 4. Figure 5(a) shows, quite dramatically, how a nonlinear self-focused beam sets off by being attracted to the interface. As this happens, energy is radiated into the linear medium. This corresponds to the fall in z_0, associated with a sharp drop in P_s/P_0, shown in Fig. 4. Figure 5(b) is the surface plot, of which Fig. 5(a) is a cross section.

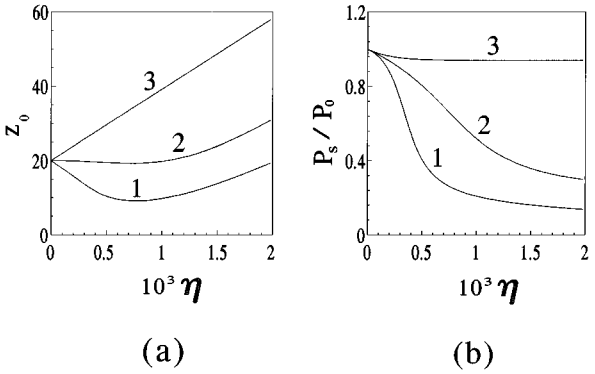

FIG. 4. Motion of the channels (self-consistent waveguides) near the interface between a linear ($\epsilon_1=2.674$) and a nonlinear ($\varepsilon_2=2.647$) medium. The initial energy is high ($u_0=2.666>u_0^*\approx 2.6602$), and there is no incident pump wave. The input coordinate is $z_0=20$, and the critical angle is 81.85°. (a) Channel trajectories. (b) Energy flow P_s normalized with the energy P_0 at $\eta=0$, along the channel trajectories. The data are (1) $(dz_0/d\eta)_0=-0.02$, (2) $(dz_0/d\eta)_0=0$, and (3) $(dz_0/d\eta)_0=0.02$.

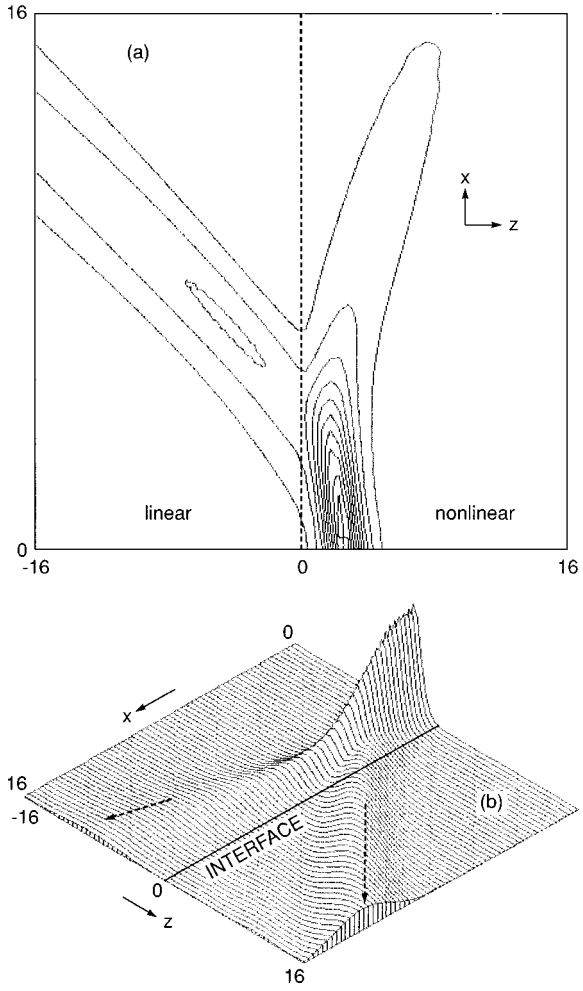

FIG. 5. Beam propagation simulation for parameters associated with curve 1 of Fig. 4. The dotted line shows the interface position. (a) Contour plot of the intensity distribution. (b) Plot of the intensity as a function of x and z.

Calculations of the motion of self-consistent waveguide channels, near the interface, can be used to explain the giant nonlinear Goos-Hänchen effect suffered by wave beams in reflection. The self-focused channels, excited during the filamentation of the beams in the vicinity of the interface [10,13], become attracted to it and provide energy transfer along the interface. This is followed by local emission into the linear medium, and it is this phenomenon that can lead to a giant shift of the center of gravity of reflected beams, with respect to incident ones.

IV. DYNAMICS OF SELF-CONSISTENT WAVEGUIDE CHANNELS INSIDE A NONLINEAR LAYER

Consider now a planar nonlinear layer of thickness $2d$, lying in the region $-d<z<d$, that is embedded in an infinite linear medium. Let the nonlinear permittivity be $\varepsilon(|E|^2)$, assume that its thickness exceeds the transverse dimension of any self-consistent channel that could be formed i.e., $2d>1/\kappa_2^{(s)}$; and, finally, let the linear permittivity be ε_2. Radiative energy losses are now possible through both boundaries of the layer, and this can lead to an interaction

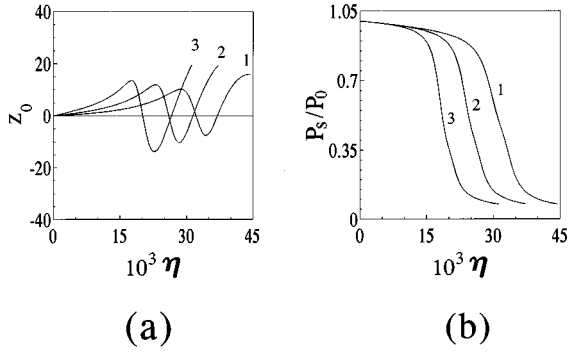

FIG. 6. Spatial dynamics of the self-consistent channels inside a layer of nonlinear material. The thickness of the layer is equal to 30 ($d=15$). The initial energy corresponds to a value $u_0=2.666$. The data are (1) $(dz_0/d\eta)_0=0.000$, (2) $(dz_0/d\eta)_0=0.0002$, and (3) $(dz_0/d\eta)_0=0.0004$. (a) Channel trajectories. (b) Normalized energy flow in the self-focused (P_s) channels.

between the interfaces. Equations (30), taking into account both interfaces, become

$$\frac{d^2z_0}{d\eta^2}=\frac{8}{3}\frac{\kappa_2^{(s)^3}}{\Delta\varepsilon}(\kappa_2^{(s)^2}-\kappa_1^{(s)^2})\sinh(2\kappa_2^{(s)}z_0)\exp(-2\kappa_2^{(s)}d), \tag{33a}$$

$$\frac{d\gamma_s}{d\eta}=-16\frac{\kappa_1^{(s)}}{\gamma_s}\frac{\kappa_2^{(s)^5}}{\Delta\varepsilon}\cosh(2\kappa_2^{(s)}z_0)\exp(-2\kappa_2^{(s)}d). \tag{33b}$$

The presence of a second boundary in the nonlinear medium leads to the possibility of the layer capturing a self-focused channel. This can occur for the case of repulsing interfaces, when $u<u_0^*$. The direct trajectory right along the middle of the layer is also a possibility. This type of solution is unstable, however, if $u>u_0^*$. Just as in the case of the single interface, the nature of the interaction with the interfaces of the layer changes during the energy loss process, and it is this that can trap channels in the nonlinear waveguide. Unfortunately, Eqs. (33) cannot be reduced as easily as was the case for Eqs. (30). This means that equations like (31) cannot be obtained here. Nevertheless, $\kappa_2^{(s)}z_0\ll x1$ for channels near the middle of layer so, for them, Eqs. (33) simplify to

$$\frac{d^2z_0}{d\eta^2}=\frac{16}{3\Delta\varepsilon}\kappa_2^{(s)^4}(\kappa_2^{(s)^2}-\kappa_1^{(s)^2})z_0\exp(-2\kappa_2^{(s)}d), \tag{34a}$$

$$\frac{du}{d\eta}=-32\frac{\kappa_2^{(s)^5}\kappa_1^{(s)}}{\Delta\varepsilon}\exp(-2\kappa_2^{(s)}d), \tag{34b}$$

where u, as before, is equal to γ_s^2. The first equation in (34), when $u<u_0^*$, describes an oscillator that has a slowly varying (along η) local spatial, frequency Ω, where

$$\Omega^2=\frac{16}{3\Delta\varepsilon}\kappa_2^{(s)^4}(\eta)[\kappa_1^{(s)^2}(\eta)-\kappa_2^{(s)^2}(\eta)]\exp[-2\kappa_2^{(s)}(\eta)d]. \tag{35}$$

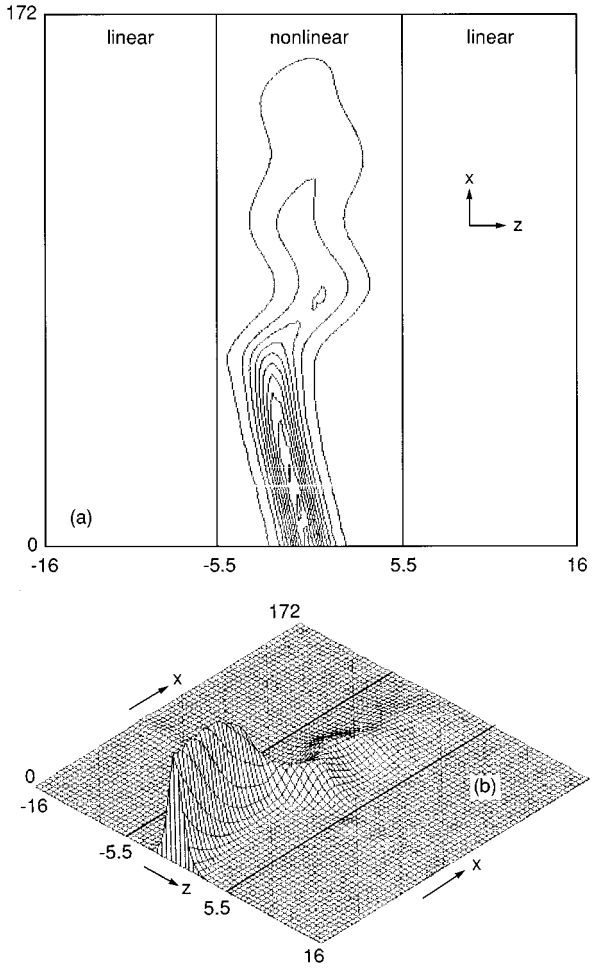

FIG. 7. Beam propagation simulation for parameters associated with curve 1 of Fig. 6. The dotted lines show the layer boundary conditions. (a) Contour plot of the intensity distribution. (b) Plot of the intensity as a function of x and z.

Ω is the spatial oscillation frequency of the channel axis near the middle of the layer, with the η-dependent functions $\kappa_{1,2}^{(s)}(\eta)$ determined by the second equation, which, incidentally, does not contain value z_0, η clearly defines the propagation length of self-focused waveguides in the layer, before total emission occurs. Figure 6(a) contains numerical calculation of typical trajectories inside the layer. All the channels displace toward one or another of the interfaces, but one of the main results is an oscillation of the channel axis around the middle of the layer. The energy changes, i.e., variations in P_s along each trajectory are displayed in Fig. 6(b).

The curves in Fig. 6 show that the self-focused channel axis oscillates around the center of the layer. As the self-focused beam moves away from the center, *in either direction*, is obvious that an interface is encountered, which then repulses the beam. As each repulsion builds up, the self-focused channel loses energy by radiation. This explains why P_s/P_0 declines, quite rapidly, as η increases. Figure 7 shows a numerical simulation of the beam behavior inside the nonlinear layer. Figure 7(a) is a contour plot of the intensity distribution, and shows the beam veering to the left or the right. Only intensities above a sensibly, yet arbitrarily, chosen low threshold are shown. This explains why P_s/P_0 drops rapidly in Fig. 6(b) as the beam appears to fade out. The radiation emitted by the nonlinear film is weak and spread over all x, so it does not show up in this graphical plot.

V. STABILITY OF HOMOGENEOUS STEADY STATES IN THE FIELD OF PLANE WAVE

The influence of the incident pump field on the dynamics of self-focused channels will now be addressed. First, the spatial stability (along x) of stationary, self-consistent channels in the field of plane electromagnetic waves will be considered. The steady state in this case is a direct channel, which is parallel to the interface [2]. In this formulation such a solution can be obtained from Eqs. (17) and (25), if the left-hand sides are set equal to zero. This takes into account the fact that, in the stationary regime, the wave numbers of the incident field and the self-consistent waveguide are equal to each other, i.e., $\gamma=\gamma_s$, and

$$\begin{aligned}&\kappa_1 A_0(-\kappa_2\sin\phi_0+\kappa_1\cos\phi_0)+\sqrt{2}\kappa_2(\kappa_2^2-\kappa_1^2)\\&\quad\times\exp(-\kappa_2 z_0)E_c=0,\\&A_0(\kappa_2\cos\phi_0+\kappa_1\sin\phi_0)-2\sqrt{2}\kappa_2^2\exp(-\kappa_2 z_0)E_c=0.\end{aligned}\tag{36}$$

Note that, since $\gamma=\gamma_s$, κ need not now be distinguished from $\kappa^{(s)}$. Solving Eq. (36) for the equilibrium phase shift ϕ_0 and the amplitude of incident wave A_0, as a function of the equilibrium channel axis position $\overline{z_0}$, gives

$$\begin{aligned}&\tan(\overline{\phi_0})=\kappa_2/\kappa_1,\\&A_0=\sqrt{2(1+\kappa_2^2/\kappa_1^2)}\,\kappa_2\exp(-\kappa_2\overline{z_0})E_c,\end{aligned}\tag{37}$$

Within the framework of these approximations, the expressions given by (37) coincide with the exact solution of the problem [2,10].

Stability, with respect to perturbations of the stationary channel position, energy flow, and phase shift can now be analyzed. First, Eqs. (17) and (25) are linearized in the neighborhood of the stationary solution and this step is followed by letting $z_0=\overline{z_0}+\delta z$, $\gamma_s=\gamma_s^{(0)}+\delta\gamma$, and $\phi=\phi_0+\delta\phi$, where δz, $\delta\gamma$, and $\delta\phi$ are small perturbations to the *equilibrium* values of the channel position, wave number and phase, respectively. If these perturbations are proportional to $e^{p\eta}$, then a set of linear characteristic equations, defining the dynamics of the channel near the steady state, can be obtained. Note that, if any part of the system experiences growth, it is unstable. In the limit of $\kappa_1\gg\kappa_2$, the characteristic equation is reduced to

$$\begin{aligned}&[(\gamma_s^{(0)}p)^2+\tfrac{4}{3}\kappa_2^4\exp(-2\kappa_2\overline{z_0})]\\&\quad\times((\gamma_s^{(0)}p)^2-4\kappa_2^4\exp(-2\kappa_2\overline{z_0}))=0.\end{aligned}\tag{38}$$

One root of Eq. (38) describes the instability with respect to perturbations in *energy and phase* that grow with the increment

$$\Gamma_E=2\kappa_2^2\exp(-\kappa_2\overline{z_0}),\tag{39}$$

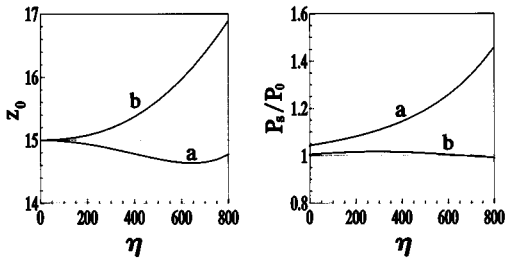

FIG. 8. Spatial channel dynamics, near the steady state, in the field of an incident plane wave (a) $\kappa_1 \gg \kappa_2$ and $\gamma_s^{(0)^2}=2.65$. (b) One example of the general case $\gamma_s^{(0)^2}=2.67$. The horizontal lines (z_0, $P_s/P_0=\text{const}$) in both figures correspond to the steady states. Initially, $z_0=\overline{z_0}=15$.

The other root of Eq. (38) describes small oscillations of the *channel* axis, around the equilibrium position, that have a wave number

$$K_c=\frac{2}{\sqrt{3}}\,\kappa_2^2\exp(-\kappa_2\overline{z_0}). \tag{40}$$

Once again, it is important to remember that, even if only one root of the characteristic equation implies growth, then the whole system is unstable.

For the other limiting case, $\kappa_1=0$, the characteristic equation gives

$$(\gamma_s^{(0)}p)^2=-\tfrac{4}{3}\kappa_2^4\exp(-2\kappa_2\overline{z_0}), \tag{41}$$

Only this case is stable, but it is not very important because it corresponds to only one point. In fact, even if $\kappa_1\approx 0$ the system is still unstable. Equation (41) describes *energy and channel axis* oscillations near a steady state, that have a wave number

$$K=\frac{2}{\sqrt{3}}\,\kappa_2^2\exp(-\kappa_2\overline{z_0}). \tag{42}$$

Using Eqs. (17) and (25), the power (P_s/P_0) and the beam center (z_0) shown as curve *a* in Fig. 8 demonstrate the rapid growth in channel energy governed by the increment in Eq. (30), and the channel axis oscillation governed by the wave number in Eq. (40). The energy is gained, of course, from the pump wave. In the general case, the characteristic equation is

$$(\gamma_s^{(0)}p)^4+b(\gamma_s^{(0)}p)^3+c(\gamma_s^{(0)}p)^2+d(\gamma_s^{(0)}p)+e=0, \tag{43}$$

where

$$b=-\frac{\gamma_s^{(0)^2}\kappa_2^3\,\exp(-2\kappa_2 z_0)}{(\gamma_s^{(0)^2}+\kappa_2^2)(\kappa_1^2+\kappa_2^2)}\left(8\kappa_1\kappa_2 z_0-12\kappa_1-4\frac{\kappa_2^2}{\kappa_1}\right),$$

$$c=\frac{8\kappa_2^4\gamma_s^{(0)^2}(\kappa_2^2-\kappa_1^2)(\gamma_s^{(0)^2}-\kappa_2^2)\exp(-2\kappa_2 z_0)}{(\kappa_2^2+\kappa_1^2)(\gamma_s^{(0)^2}+\kappa_2^2)(3\gamma_s^{(0)^2}-\kappa_2^2)},$$

$$d=\frac{16\kappa_2^7\gamma_s^{(0)^4}\exp(-4\kappa_2 z_0)}{\kappa_1(3\gamma_s^{(0)^2}-\kappa_2^2)(\gamma_s^{(0)^2}+\kappa_2^2)},$$

$$e=-\frac{16\kappa_2^8\gamma_s^{(0)^4}\exp(-4\kappa_2 z_0)}{(3\gamma_s^{(0)^2}-\kappa_2^2)(\kappa_2^2+\gamma_s^{(0)^2})}.$$

Equation (43), being a quartic equation, has four solutions, which are equal to the four solutions of the following pair of quadratic equations:

$$x^2+(b+\sqrt{8y+b^2-4c})\,\frac{x}{2}+\left(y+\frac{by-d}{\sqrt{8y+b^2-4c}}\right)=0, \tag{44a}$$

$$x^2+(b-\sqrt{8y+b^2-4c})\,\frac{x}{2}+\left(y-\frac{by-d}{\sqrt{8y+b^2-4c}}\right)=0, \tag{44b}$$

Here y is any one of the *real* solutions of the following cubic equation:

$$8y^3-4cy^2+(2bd-8e)y+e(4c-b^2)-d^2=0.$$

For $\varepsilon_1=2.674$ and $\varepsilon_2=2.647$, a plot of the four solutions of Eq. (43), versus $\gamma_s^{(0)^2}$, is displayed in Fig. 9. This figure emphasizes further that, even in the general case, instability ensues because of the appearance of real parts in the roots, i.e., the general case has not changed the conclusion drawn from Eq. (38). Curves *b*, shown in Fig. 8, give the growth of the channel axis z_0 and the oscillation of the channel power P_s/P_0 for $\gamma_s^{(0)^2}=2.67$. The runaway growth of z_0 means that the self-focused channel moves rapidly away from its initial position and does not, on average, capture any more energy. The results just given concerning the stability of self-consistent waveguide channels confirm the conclusions obtained in the recent paper by Aliev *et al.* [10] that were based upon energy considerations.

VI. DYNAMICS OF SELF-SUSTAINING WAVEGUIDE CHANNELS IN THE FIELD OF WIDE INCIDENT BEAMS

The results of a numerical study of the dynamics of self-focused waveguide channels that exist in the field of incident *wide beams* will now be presented. The method is based, once again, upon Eqs. (17) and (25), together with the additional phase shift equation

$$\frac{d\phi}{dx}=\gamma_s-\gamma. \tag{45}$$

The amplitude distribution of the beam field, at the interface, is

$$A_0(x)=\begin{cases} A_0^m\left(1-\dfrac{(x-b)^2}{b^2}\right)^2, & 0<x<2b \\ 0, & x<0,\ x>2b, \end{cases} \tag{46}$$

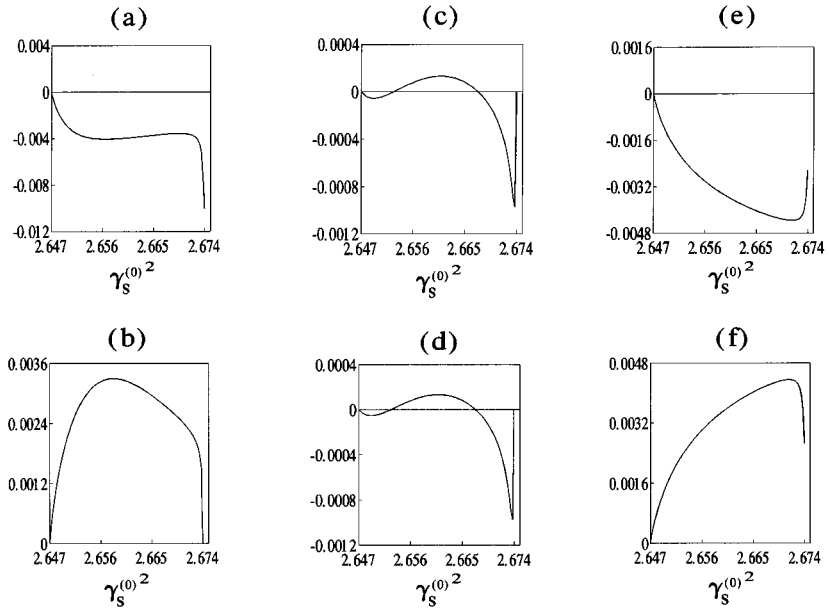

FIG. 9. Solutions (ordinates) of Eq. (43) vs $\gamma_s^{(0)^2}$ (abscissae) for $\varepsilon_1=2.674$ and $\varepsilon_2=2.647$. (a), (b), (c), and (d) show the real parts of the solutions, because the imaginary parts of the first two solutions are zero. (e) and (f) show the imaginary parts of the remaining two roots.

where A_0^m is the maximum value of the field of incident beam and b is the half-width of an illuminated spot at the interface. The phase front of the incident beam is assumed to be a plane. Also, γ_s will be allowed to have values greater than ϵ_1 which permits a change in the nonlinear mode from radiative to nonradiative. This can be caused by energy transfer from the pump wave to the channel. In order to satisfy the radiation conditions, when the sign of the expression under the square root in $\kappa_1^{(s)}$ changes in Eqs. (17) and (25), the substitution $\kappa_t^{(s)} \rightarrow i\kappa_1^{(s)}$ is performed. This provides the exponential decrease of the correction to the field $E_1^{(0)}$, where $z \rightarrow \infty$.

Some numerical results of calculations are presented in Fig. 10, in which the value b, in dimensionless units, has been set equal to 400. In Fig. 10(a) trajectories of the self-consistent waveguide channels, with an initial value $u_0=2.655$, and an initial position $z_0=15$, $(dz_0/d\eta)_0=0$, are shown. In the course of the calculation, z_0 must be selected and, from a previous section on plane wave pumping, this same z_0 determines the *plane wave amplitude* $\overline{A_0}$ that would be needed to maintain it. A_0 has been calculated, therefore, and used to normalize A_0^m, as stated in the caption. It can be seen that channel trajectories can go deep into the nonlinear medium, which occurs either with the loss of some part of the total energy, with some increase, or with total emission. This is caused by phase relations between the incident field and the field of the self-consistent waveguide. These relations change, generally, along the track of the propagation. Depending upon the value of this phase shift, the external field can accomplish either a positive work contribution to the channel field, which leads to the partial compensation of its radiative losses, or negative work, leading to an increase of the radiative losses.

The well-known possibility [4,13] that a giant nonlinear Goos-Hänchen shift of the intensity maximum of the reflected signal, through a value much greater than the incident beam width, is strikingly shown in Fig. 11. A Goos-Hänchen shift means that if a beam is incident on a dielectric surface then the center of the reflected beam does not appear to come from the point of impact of the center of the incoming beam. Nonlinearity exaggerates this effect, leading to the so-called

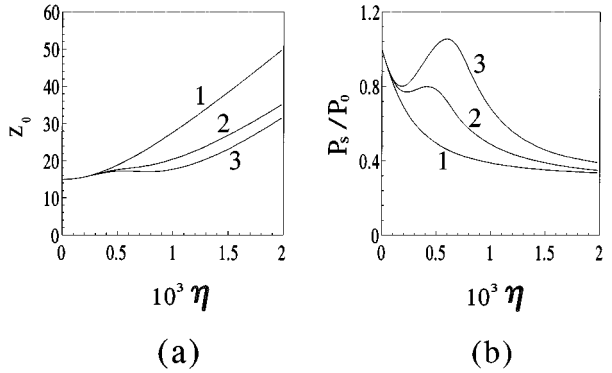

FIG. 10. Spatial channel dynamics and normalized energy flow along the trajectories in the field of an incident wave beam [see Eq. (35)], for half-width $b=400$; $\gamma^2=2.655$, $z_0=15$; and $(dz_0/d\eta)_0=0$, $\phi_0=0.57$ (initial phase shift). (1) $A_0^m/A_0=k=0.0$. (2) $k=1.2$. (3) $k=1.6$.

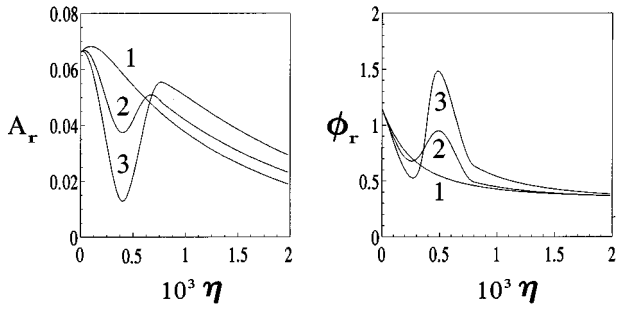

FIG. 11. The demonstration of the development of a giant nonlinear Goos-Hänchen effect. $b=400$. $\gamma^2=2.655$. $\phi_0=\phi$. (1) $k=0.0$, (2) $k=0.6$. (3) $k=1.2$. A_r is the reflected amplitude and ϕ_r is the phase change.

giant effect. In Fig. 11 curve 1 is a clear cut case, in so far as the peak of $|A_r|^2$ (reflected intensity) occurs at $\eta \neq 0$. Curves 2 and 3 are more dramatic, and the shift can be measured from $\eta=0$ to some average position $\eta \neq 0$, where the bulk of the reflected energy appears to be coming from. Its explanation lies in the resonant interaction of the beam field with the excited self-focused channel in the nonlinear medium in the near-surface region. Such interaction of self-consistent waveguides with electromagnetic beams can be used for the control of the channel field structure, and their behavior, in the nonlinear medium, by the radiation fields.

VII. CONCLUSION

In conclusion, a perturbation theory is presented that describes, quantitatively, the interaction of wave fields with radiatively damped self-focused channels near the interface between linear and nonlinear media, under the condition of small overlap. This approach is valid, under certain conditions, for a wide range of other problems, where coupling between radiation and quasilocalized eigenmodes must be accounted for. By means of this theory, an investigation of a number of effects is shown to be possible. These include the interaction of self-consistent channels with an interface and an incident wide electromagnetic beam. The approach given is instructive because the mathematical theory permits an interpretation, and an understanding, from a physical point of view, of certain interesting phenomena. It is clear that nonperturbative regimes will still need numerical analysis, but the *numerical* conclusions reported by Tomlinson *et al.* [13], are, nevertheless, generated by the analysis reported here. It is believed that the approach here will be very helpful in the study of the stability of nontrivial nonlinear structures, and that it will lead to a large number of applications in more than one discipline.

ACKNOWLEDGMENTS

We should like to thank M. D. Chernobrovtseva for performing some of early numerical calculations. A. D. Boardman and K. Xie acknowledge support from the UK Engineering and Physical Sciences Research Council (EPSRC).

[1] A. E. Kaplan, Pis'ma Zh. Eksp. Teor. Fiz. **24**, 132 (1976) [JETP Lett. **24**, 114 (1976)].
[2] A. E. Kaplan, Zh. Eksp. Teor. Fiz. **72**, 1710 (1977) [Sov. Phys. JETP **45**, 896 (1977)].
[3] A. E. Kaplan, IEEE J. Quantum Electron. **QE-17**, 336 (1981).
[4] A. E. Kaplan, P. W. Smith, and W. J. Tomlinson, in *Nonlinear Waves in Solid State Physics*, Vol. 247 of *NATO Advanced Study Institute, Series B: Physics*, edited by A. D. Boardman *et al.* (Plenum, New York, 1990), p. 93.
[5] A. E. Kaplan, Kuant. Elektron (Moscow) **5**, 166 (1978); Sov. J. Quantum Electron **8**, 95 (1978).
[6] A. E. Kaplan, Radiophys. Quantum Electron. **22**, 229 (1981).
[7] P. W. Smith, J. P. Hermann, W. J. Tomlinson, and P. J. Maloney, Appl. Phys. Lett. **35**, 846 (1979).
[8] V. I. Bespalov and V. I. Talanov, Pis'ma Zh. Eksp. Teor. Fiz. **3**, 471 (1966) [JETP Lett. **3**, 307 (1966)].
[9] A. A. Kolokolov and A. I. Sukov, Izv. Vyssh. Vchebn. Zaved. Radiofiz. **21**, 1459 (1978) [Sov. Radiophysics **21**, 1013 (1978)].
[10] Yu. M. Aliev, A. D. Boardman, K. Xie, and A. A. Zharov, Phys. Rev. E **49**, 1624 (1994).
[11] D. Marcuse, Appl. Opt. **19**, 3130 (1980).
[12] N. N. Rozanov, Opt. Spektrosk. **47**, 606 (1979) [Opt. Spectrosc. (USSR) **47**, 335 (1979)].
[13] W. G. Tomlinson, J. P. Gordon, P. W. Smith, and A. E. Kaplan, Appl. Opt. **12**, 2041 (1982).
[14] N. N. Akhmediev, V. I. Korneev, and V. V. Kuz'menko, Zh. Eksp. Teor. Fiz. **88**, 107 (1985) [Sov. Phys. JETP **61**, 62 (1985)].
[15] L. M. Brekhovskikh, *Waves in Layered Media* (Academic, New York, 1980).
[16] B. R. Horovitz and T. Tamir, J. Opt. Soc. Am. **61**, 586 (1971).
[17] Ya. L. Bogomolov, A. V. Kochetov, A. G. Litvak, and V. A. Mironov, Zh. Eksp. Teor. Fiz. **98**, 1191 (1990) [Sov. Phys. JETP **71**, 667 (1990)].
[18] A. G. Litvak and V. A. Mironov, Radiofiz **11**, 1911 (1968).
[19] V. S. Agranovich, V. Babichenko, and V. Ya. Chernyak, Pis'ma Zh. Eksp. Teor. Fiz. **32**, 532 (1980) [Sov. Phys. JETP Lett. **32**, 512 (1981)].
[20] A. D. Boardman, P. Egan, F. Lederer, U. Langbein, and D. Mihalache, in *Nonlinear Surface Electromagnetic Phenomena*, edited by H. E. Ponath and G. I. Stegeman (North-Holland, Amsterdam, 1991), p. 73.
[21] A. D. Boardman and P. Egan, IEEE J. Quantum Electron. **QE-21**, 1701 (1985).
[22] A. D. Boardman, P. Egan, T. Twardowski, and M. Wilkins, in *Nonlinear Waves in Solid State Physics* (Ref. [4]), p. 1.
[23] L. A. Nesterov, Opt. Spektrosk. **64**, 1166 (1988) [Opt. Spectrosc. (USSR) **64**, 694 (1988)].
[24] A. V. Aceves, J. M. Moloney, and A. C. Newell, Phys. Rev. A **38**, 1809 (1989); **38**, 1828 (1989).
[25] A. B. Aceves, P. Varatharajah, A. C. Newell, E. M. Wright, G. I. Stegeman, D. R. Heatley, J. V. Moloney, and H. Adachihara, J. Opt. Soc. Am. B **7**, 963 (1990).
[26] Yu. S. Kivshar, A. M. Kosevich, and O. A. Chubykalo, Phys. Rev. A **41**, 1677 (1990).
[27] A. I. Smirnov and G. M. Fraiman, Physica D **52**, 2 (1991).
[28] Boris A. Malomed, Phys. Rev. E **47**, 2874 (1993).
[29] Yuri S. Kivshar and Boris A. Malomed, Rev. Mod. Phys. **61**, 763 (1989).
[30] V. I. Karpman and V. V. Solovjev, Physica D **3**, 481 (1981).